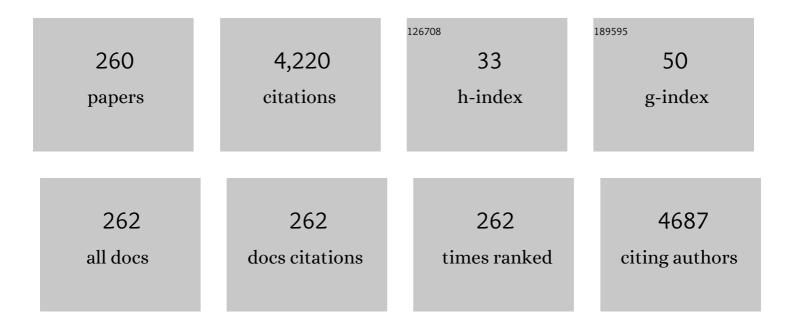
List of Publications by Year in descending order

Source: https://exaly.com/author-pdf/1580740/publications.pdf Version: 2024-02-01



AKDAINS ALL LIMAD

#	Article	IF	CITATIONS
1	Nanocomposite design of graphene modified TiO2 for electrochemical sensing in phenol detection. Korean Journal of Chemical Engineering, 2022, 39, 209-215.	1.2	16
2	Palladium selenide as cathode for dye-sensitized solar cell: Effect of palladium content. Solid-State Electronics, 2022, 190, 108255.	0.8	5
3	Synthesis of standing ZnO nanosheets and impact of Ag nanoparticles loading on its optical property. Bulletin of Materials Science, 2022, 45, 1.	0.8	1
4	Effect of potassium precursor concentration on the performance of perovskite-sensitized solar cells. Bulletin of Materials Science, 2022, 45, .	0.8	3
5	Photoelectrocatalysis Response with Synthetic Mn–N–TiO2/Ti Electrode for Removal of Rhodamine B Dye. Surface Engineering and Applied Electrochemistry, 2022, 58, 125-134.	0.3	5
6	Propylene Glycol Directed Synthesis of Silver Nanowires for Transparent Conducting Electrode Application. Journal of Electronic Materials, 2022, 51, 5150-5158.	1.0	1
7	Perovskite-sensitized solar cell utilizing TiO2 nanograss: Effect of dipping time of CH3NH3PbI3 perovskite. Journal of the Indian Chemical Society, 2022, 99, 100562.	1.3	0
8	Crystal growth and catalytic properties of AgPt and AuPt bimetallic nanostructures under surfactant effect. Inorganic Chemistry Communication, 2022, 143, 109737.	1.8	2
9	Tuning the photocatalytic activity of nanocomposite ZnO nanorods by shape-controlling the bimetallic AuAg nanoparticles. Applied Surface Science, 2021, 536, 147847.	3.1	22
10	On the performance of polymer-inorganic perovskite oxide composite light-emitting diodes: The effect of perovskite SrTiO3 additives. Nanomaterials and Nanotechnology, 2021, 11, 184798042098777.	1.2	2
11	NickelPalladium alloy–reduced graphene oxide as counter electrode for dye-sensitized solar cells. Journal of Molecular Liquids, 2021, 326, 115289.	2.3	18
12	Effect of hexamethylenetetramine surfactant in morphology and optical properties of TiO2 nanoparticle for dye-sensitized solar cells. Journal of Physics: Conference Series, 2021, 1899, 012045.	0.3	2
13	Synthesis of Large-Scale Cadmium Oxide Nanowires from an Aqueous Solution. Journal of Electronic Materials, 2021, 50, 5553-5556.	1.0	1
14	Charge transfer uplift in dye-sensitized solar cells using fibrous nanocrystals of platinum-based bimetallic counter electrodes. Surfaces and Interfaces, 2021, 26, 101311.	1.5	6
15	Two-dimensional crystal growth in ZnO nanostructures directed by poly vinylpyrrolidone. Materials Letters, 2021, 304, 130649.	1.3	3
16	Photoelectrical Dynamics Uplift in Perovskite Solar Cells by Atoms Thick 2D TiS ₂ Layer Passivation of TiO ₂ Nanograss Electron Transport Layer. ACS Applied Materials & Interfaces, 2021, 13, 3051-3061.	4.0	21
17	Comparative study of dye-sensitized solar cell utilizing selenium and palladium cathode. Journal of the Indian Chemical Society, 2021, 99, 100289.	1.3	2
18	Dye-sensitized solar cell utilizing silver doped reduced graphene oxide films counter electrode: Influence of annealing temperature on its performance. Arabian Journal of Chemistry, 2020, 13, 3383-3390.	2.3	11

#	Article	IF	CITATIONS
19	TiO2 Coated-Asphalt Buton Photocatalyst for High-Performance Motor Vehicles Gas Emission Mitigation. Emission Control Science and Technology, 2020, 6, 28-36.	0.8	7
20	Enhanced Charge Transfer in Atomâ€Thick 2H–WS ₂ Nanosheets' Electron Transport Layers of Perovskite Solar Cells. Solar Rrl, 2020, 4, 2000260.	3.1	26
21	Photoelectrical properties of anatase TiO2 with different morphologies under Au plasmonic effect. Applied Physics A: Materials Science and Processing, 2020, 126, 1.	1.1	1
22	A two-dimensional crystal growth in anatase titania nanostructures driven by trigonal hydronium ions. RSC Advances, 2020, 10, 16886-16891.	1.7	3
23	Influence of annealing temperature of ZnS-coated TiO2 films on the performance of dye-sensitized solar cells. Optik, 2020, 211, 164644.	1.4	5
24	Dependence of optical properties of Mg-doped ZnO nanorods on Al dopant. Surfaces and Interfaces, 2020, 19, 100518.	1.5	15
25	The influence of MoSe2 coated onto Pt film to DSSC performance with the structure TiO2/Dye/LxMoSe2Pt (0Ââ‰ÅxÂâ‰Å5). Materials Letters, 2020, 275, 128076.	1.3	7
26	Ultra-thin MoS2 nanosheet for electron transport layer of perovskite solar cells. Optical Materials, 2020, 104, 109933.	1.7	24
27	Effect of annealing treatment on multilayer TiO2 films on the performance of dye-sensitized solar cells. Optik, 2020, 218, 164976.	1.4	13
28	Enhancing the interfacial carrier dynamic in perovskite solar cells with an ultra-thin single-crystalline nanograss-like TiO ₂ electron transport layer. Journal of Materials Chemistry A, 2020, 8, 13820-13831.	5.2	12
29	Optical, structural and morphological studies of TiO2 thin film synthesized by liquid phase deposition method. AIP Conference Proceedings, 2020, , .	0.3	0
30	Fabrication of Pt-Pd@ITO grown heterogeneous nanocatalyst as efficient remediator for toxic methyl parathion in aqueous media. Environmental Science and Pollution Research, 2020, 27, 9970-9978.	2.7	11
31	Enhanced visible light-driven photocatalytic degradation supported by Au-TiO2 coral-needle nanoparticles. Journal of Photochemistry and Photobiology A: Chemistry, 2020, 398, 112589.	2.0	23
32	Micro-strain effect on electronic properties in graphene induced by silver nanowires. Physica E: Low-Dimensional Systems and Nanostructures, 2020, 123, 114203.	1.3	2
33	Seed-Mediated Synthesis and Photoelectric Properties of Selenium Doped Zinc Oxide Nanorods. Sains Malaysiana, 2020, 49, 3055-3063.	0.3	5
34	Liquid Phase Deposition of TiO2 Films for Electron Transport Layer of Perovskite Solar Cells. Journal of Nano- and Electronic Physics, 2020, 12, 03019-1-03019-5.	0.2	0
35	Chalcogenide material as high photoelectrochemical performance Se doped TiO ₂ /Ti electrode: Its application for Rhodamine B degradation. Journal of Physics: Conference Series, 2019, 1242, 012016.	0.3	15
36	Fibrous bimetallic silver palladium and ruthenium palladium nanocrystals exhibitÂan exceptionally high active catalytic process in acetone hydrogenation. Materials Today Chemistry, 2019, 14, 100178.	1.7	3

#	Article	IF	CITATIONS
37	Highly efficient planar perovskite solar cells <i>via</i> acid-assisted surface passivation. Journal of Materials Chemistry A, 2019, 7, 22323-22331.	5.2	34
38	Improvement of dye-sensitized solar cell performance by utilizing graphene-coated TiO2 films photoanode. Superlattices and Microstructures, 2019, 128, 92-98.	1.4	20
39	TiO2–SrTiO3 composite photoanode: effect of strontium precursor concentration on the performance of dye-sensitized solar cells. Applied Physics A: Materials Science and Processing, 2019, 125, 1.	1.1	19
40	Highly sensitive fipronil pesticide detection on ilmenite (FeO.TiO2)-carbon paste composite electrode. Surfaces and Interfaces, 2019, 16, 108-113.	1.5	43
41	Facile charge transfer in fibrous PdPt bimetallic nanocube counter electrodes. New Journal of Chemistry, 2019, 43, 11148-11156.	1.4	5
42	Effect of Silver Concentration towards Formationof AgPt Nanofernfilms as SERS Substrates. Materials Science Forum, 2019, 948, 231-236.	0.3	2
43	Zinc sulphide-coated titanium dioxide films as photoanode for dye-sensitized solar cells: Effect of immersion time on its performance. Superlattices and Microstructures, 2019, 130, 153-159.	1.4	13
44	Enhanced charge transfer activity in Au nanoparticles decorated ZnO nanorods photoanode. Physica E: Low-Dimensional Systems and Nanostructures, 2019, 111, 44-50.	1.3	19
45	Synthesis and electrochemical performance of graphene-TiO2-carbon paste nanocomposites electrode in phenol detection. Journal of Physics and Chemistry of Solids, 2019, 131, 104-110.	1.9	38
46	Humidity effect on photoelectrical properties of photosensitive field effect transistors. Organic Electronics, 2019, 69, 42-47.	1.4	1
47	Leadâ€Free Cs ₂ BiAgBr ₆ Double Perovskiteâ€Based Humidity Sensor with Superfast Recovery Time. Advanced Functional Materials, 2019, 29, 1902234.	7.8	143
48	Dye-sensitized solar cell utilizing TiO2–sulphur composite photoanode: influence of sulphur precursor content. SN Applied Sciences, 2019, 1, 1.	1.5	4
49	Thermal impact on (001) faceted anatase TiO2 microtablets and nanowalls's lattices and its effect on the photon to current conversion efficiency. Journal of Physics and Chemistry of Solids, 2019, 127, 213-223.	1.9	4
50	Bimetallic AuAg sharp-branch mesoflowers as catalyst for hydrogenation of acetone. Materials Chemistry and Physics, 2019, 225, 443-450.	2.0	19
51	High performance cypermethrin pesticide detection using anatase TiO2-carbon paste nanocomposites electrode. Microchemical Journal, 2019, 145, 756-761.	2.3	55
52	Reka Bentuk Sensor Pendar Cahaya Bintik Kuantum ZnCdSe untuk Mengesan Racun Perosak. Sains Malaysiana, 2019, 48, 1513-1518.	0.3	2
53	Two-Dimensional, Hierarchical Ag-Doped TiO ₂ Nanocatalysts: Effect of the Metal Oxidation State on the Photocatalytic Properties. ACS Omega, 2018, 3, 2579-2587.	1.6	59
54	Perovskite-sensitized solar cells-based Ga–TiO2 nanodiatom-like photoanode: the improvement of performance by perovskite crystallinity refinement. Applied Physics A: Materials Science and Processing, 2018, 124, 1.	1.1	13

#	Article	IF	CITATIONS
55	Effect of hexamethylenetetramine (HMT) concentration on the properties of boron doped ZnO nanotubes array films and the performance of dye-sensitized solar cell (DSSC). AIP Conference Proceedings, 2018, , .	0.3	2
56	Hydrothermally grown of well-aligned ZnONRs: dependence of alignment ordering upon precursor concentration. Journal of Materials Science: Materials in Electronics, 2018, 29, 6892-6897.	1.1	11
57	Mn-doping-induced photocatalytic activity enhancement of ZnO nanorods prepared on glass substrates. Applied Surface Science, 2018, 439, 285-297.	3.1	131
58	Dye-sensitized solar cell utilizing silver-reduced graphene oxide film counter electrode: effect of silver content on its performance. Ionics, 2018, 24, 3665-3671.	1.2	14
59	Dye-Sensitized Solar Cell Utilizing TiO2 Nanostructure Films: Effect of Synthesis Temperature. Russian Journal of Electrochemistry, 2018, 54, 56-61.	0.3	6
60	Advances in porous and high-energy (001)-faceted anatase TiO2 nanostructures. Optical Materials, 2018, 75, 390-430.	1.7	30
61	Geant4 Step towards the Durability and Smooth Response of Silicon Based Neutron Dosimeter, and Protection from Thermal Neutrons. , 2018, , .		0
62	Effect of N719 Dye Dipping Temperature on the Performance of Dye-Sensitized Solar Cell. Russian Journal of Electrochemistry, 2018, 54, 755-759.	0.3	8
63	Effect of Annealing Temperature of Gold Doped Reduced Graphene Oxide Counter Electrode on the Performance of Dye-sensitized Solar Cell. International Journal of Electrochemical Science, 2018, 13, 5620-5629.	0.5	3
64	Optimum growth time in AgPt nanofern preparation for enhancement of surface-enhanced Raman scattering intensity. Advances in Natural Sciences: Nanoscience and Nanotechnology, 2018, 9, 045012.	0.7	1
65	Hierarchical Bimetallic AgPt Nanoferns as High-Performance Catalysts for Selective Acetone Hydrogenation to Isopropanol. ACS Omega, 2018, 3, 11526-11536.	1.6	15
66	Structural and properties transformation in ZnO hexagonal nanorod by ruthenium doping and its effect on DSSCs power conversion efficiency. Superlattices and Microstructures, 2018, 123, 119-128.	1.4	19
67	TiO2-coated ZnS films as photoanode for dye-sensitized solar cell: effect of zinc nitrate hexahydrate concentration on the performance. Applied Physics A: Materials Science and Processing, 2018, 124, 1.	1.1	10
68	Effect of surface density silver nanoplate films toward surface-enhanced Raman scattering enhancement for bisphenol A detection. Journal of Physics: Conference Series, 2018, 985, 012026.	0.3	0
69	Synthesis of white fluorescent pyrrolic nitrogen-doped graphene quantum dots. Optical Materials, 2018, 83, 306-314.	1.7	33
70	Dyeâ€sensitised solar cell utilising gold doped reduced graphene oxide counter electrode: influence of annealing time. Micro and Nano Letters, 2018, 13, 1224-1226.	0.6	2
71	Urea and creatinine detection on nano-laminated gold thin film using Kretschmann-based surface plasmon resonance biosensor. PLoS ONE, 2018, 13, e0201228.	1.1	57
72	Dye-sensitized Solar Cell utilizing Gold Doped Reduced Graphene Oxide Films Counter Electrode. Journal of New Materials for Electrochemical Systems, 2018, 21, 113-117.	0.3	7

#	Article	IF	CITATIONS
73	Comparative study of the properties of TiO2 nanoflower and TiO2-ZnO composite nanoflower and their application in dye-sensitized solar cells. Ionics, 2017, 23, 1897-1902.	1.2	14
74	Green synthesis of few-layered graphene from aqueous processed graphite exfoliation for graphene thin film preparation. Materials Chemistry and Physics, 2017, 193, 212-219.	2.0	75
75	SiO2 caped Fe3O4 nanostructures as an active heterogeneous catalyst for 4-nitrophenol reduction. Microsystem Technologies, 2017, 23, 5745-5758.	1.2	43
76	Synthesis of two-dimensional nanowall of Cu-Doped TiO 2 and its application as photoanode in DSSCs. Physica E: Low-Dimensional Systems and Nanostructures, 2017, 91, 185-189.	1.3	61
77	Design and measurement technique of surface-enhanced Raman scattering for detection of bisphenol A. Advances in Natural Sciences: Nanoscience and Nanotechnology, 2017, 8, 025008.	0.7	9
78	High figure of merit transparent conducting Sb-doped SnO 2 thin films prepared via ultrasonic spray pyrolysis. Journal of Alloys and Compounds, 2017, 720, 79-85.	2.8	59
79	Comparative trial of saccharin-added electrolyte for improving the structure of an electrodeposited magnetic FeCoNi thin film. Thin Solid Films, 2017, 642, 51-57.	0.8	24
80	Detection of creatinine on triangular silver nanoplates surface using surface-enhanced Raman scattering sensor. International Journal of Biomedical Nanoscience and Nanotechnology, 2017, 3, 335.	0.1	3
81	Scalable Mesoporous Platinum Diselenide Nanosheet Synthesis in Water. ACS Omega, 2017, 2, 3325-3332.	1.6	32
82	Influence of ZnO growth temperature on the performance of dye-sensitized solar cell utilizing TiO2-ZnO composite film photoanode. Ionics, 2017, 23, 3533-3544.	1.2	10
83	Dye-sensitized solar cell (DSSC) utilizing reduced graphene oxide (RGO) films counter electrode: effect of graphene oxide (GO) content. Journal of Materials Science: Materials in Electronics, 2017, 28, 1674-1678.	1.1	18
84	Direct deposition of silver nanoplates on quartz surface by sequence pre-treatment hydroxylation and silanisation. MethodsX, 2017, 4, 486-491.	0.7	5
85	Influence of Ag ion adsorption on the photoactivity of ZnO nanorods for dye-sensitized solar cell application. Materials Express, 2017, 7, 312-318.	0.2	14
86	Gold Nanoplates for a Localized Surface Plasmon Resonance-Based Boric Acid Sensor. Sensors, 2017, 17, 947.	2.1	30
87	Effect of Spin-Coating Cycle on the Properties of TiO2 Thin Film and Performance of DSSC. International Journal of Electrochemical Science, 2017, 12, 5529-5538.	0.5	22
88	Synthesis of silver–platinum nanoferns substrates used in surface-enhanced Raman spectroscopy sensors to detect creatinine. Advances in Natural Sciences: Nanoscience and Nanotechnology, 2017, 8, 025015.	0.7	4
89	TiO2-BaTiO3 Composite Films as Photoanode for Dye Sensitized Solar Cell: Effect of BaTiO3 Content. Journal of New Materials for Electrochemical Systems, 2017, 20, 109-113.	0.3	3
90	Graphene Growth at Low Temperatures using RF-Plasma Enhanced Chemical Vapour Deposition. Sains Malaysiana, 2017, 46, 1111-1117.	0.3	12

#	Article	IF	CITATIONS
91	Dye-sensitized Solar Cell (DSSC) Utilizing TiO2 Films Prepared via Microwave Irradiation Technique: Effect of TiO2 Growth Time. Journal of New Materials for Electrochemical Systems, 2017, 20, 059-064.	0.3	1
92	Multi-cycle Growth of Boron Doped ZnO Films as Photoanode for Dye-Sensitized Solar Cell (DSSC). International Journal of Electrochemical Science, 2016, 11, 10965-10977.	0.5	4
93	Configurable impedance matching to maximise power extraction for enabling self-powered system based-on photovoltaic cells. Electronic Materials Letters, 2016, 12, 545-550.	1.0	2
94	Room temperature photoluminescence properties of ZnO nanorods grown by hydrothermal reaction. AIP Conference Proceedings, 2016, , .	0.3	12
95	Effect of growth solution concentration on the performance of gallium doped ZnO nanostructures dye sensitized solar cells (DSSCs). AIP Conference Proceedings, 2016, , .	0.3	4
96	Porous (001)-faceted anatase TiO ₂ nanorice thin film for efficient dye-sensitized solar cell. EPJ Photovoltaics, 2016, 7, 70501.	0.8	15
97	Fibrous AuPt bimetallic nanocatalyst with enhanced catalytic performance. RSC Advances, 2016, 6, 27696-27705.	1.7	16
98	Fibrous platinum nanocubes modified indium tin oxide electrodes for effective electrooxidation of alcohols and sensitive detection of hydrazine. Journal of Electroanalytical Chemistry, 2016, 779, 156-160.	1.9	5
99	Boron doped ZnO films for dye-sensitized solar cell (DSSC): effect of annealing temperature. Journal of Materials Science: Materials in Electronics, 2016, 27, 8394-8401.	1.1	5
100	Composition dependence of photoluminescence properties of poly(9,9-di- n -hexylfluorenyl-2,7-diyl) with perovskite-structured SrTiO 3 nanocomposites. Superlattices and Microstructures, 2016, 93, 153-156.	1.4	3
101	Effect of dimethyl borate composition on the performance of boron doped ZnO dye-sensitized solar cell (DSSC). Journal of Materials Science: Materials in Electronics, 2016, 27, 2228-2234.	1.1	6
102	Synthesis of crystalline perovskite-structured SrTiO3 nanoparticles using an alkali hydrothermal process. International Journal of Minerals, Metallurgy and Materials, 2016, 23, 109-115.	2.4	10
103	Characterization and Fabrication of Nanocomposite Thin Films of PANI Embedded with Ag-Mn Alloy for E. coli Sensor. Materials Today: Proceedings, 2016, 3, 538-544.	0.9	5
104	Efficient quantum capacitance enhancement in DSSC by gold nanoparticles plasmonic effect. Electrochimica Acta, 2016, 195, 134-142.	2.6	46
105	Synthesis of defect-rich, (001) faceted-ZnO nanorod on a FTO substrate as efficient photocatalysts for dehydrogenation of isopropanol to acetone. Journal of Physics and Chemistry of Solids, 2016, 93, 73-78.	1.9	13
106	(001) faceted-Ga-TiO2 microtablet synthesis and its organic perovskite sensitized solar cells characterization. Journal of Alloys and Compounds, 2016, 674, 470-476.	2.8	16
107	Enhanced thermoelectric properties of bismuth telluride–organic hybrid films via graphene doping. Applied Physics A: Materials Science and Processing, 2016, 122, 1.	1.1	9
108	Microwave-assisted hydrolysis preparation of highly crystalline ZnO nanorod array for room temperature photoluminescence-based CO gas sensor. Sensors and Actuators B: Chemical, 2016, 227, 304-312.	4.0	75

#	Article	IF	CITATIONS
109	Electroluminescence Enhancement of Polymer Light Emitting Diodes Through Surface Plasmons by Ag Nanoplates. Acta Physica Polonica A, 2016, 129, 711-713.	0.2	2
110	Self-Assembly of High Density of Triangular Silver Nanoplate Films Promoted by 3-Aminopropyltrimethoxysilane. Applied Sciences (Switzerland), 2015, 5, 209-221.	1.3	32
111	Thermal Annealing Effect on Structural, Morphological, and Sensor Performance of PANI-Ag-Fe Based ElectrochemicalE. coliSensor for Environmental Monitoring. Scientific World Journal, The, 2015, 2015, 1-8.	0.8	8
112	Effect of growth temperature and time on the ZnO film properties and the performance of dye-sensitized solar cell (DSSC). Journal of Solid State Electrochemistry, 2015, 19, 1217-1221.	1.2	14
113	Effect of boric acid composition on the properties of ZnO thin film nanotubes and the performance of dye-sensitized solar cell (DSSC). Journal of Alloys and Compounds, 2015, 648, 86-91.	2.8	24
114	Porous Zn-doped TiO2 nanowall photoanode: Effect of Zn2+ concentration on the dye-sensitized solar cell performance. Applied Surface Science, 2015, 353, 835-842.	3.1	42
115	Influence of optical band gap and particle size on the catalytic properties of Sm/SnO2–TiO2 nanoparticles. Superlattices and Microstructures, 2015, 82, 234-247.	1.4	58
116	Synthesis and characterization of TiO2–ZnO core–shell nanograss hetero-structure and its application in dye-sensitized solar cell (DSSC). Journal of Materials Science: Materials in Electronics, 2015, 26, 4936-4943.	1.1	5
117	Synthesis of Amorphous Platinum Nanofibers Directly on an ITO Substrate and Its Heterogeneous Catalytic Hydrogenation Characterization. ACS Applied Materials & Interfaces, 2015, 7, 7776-7785.	4.0	23
118	Morphological, optical, structural and photoelectrochemical properties of TiO2nanoflower prepared via PVP surfactant assisted liquid phase deposition technique. Journal of Experimental Nanoscience, 2015, 10, 925-936.	1.3	4
119	Effect of surfactant on the physical properties of ZnO nanorods and the performance of ZnO photoelectrochemical cell. Journal of Experimental Nanoscience, 2015, 10, 599-609.	1.3	20
120	Selective Heterogeneous Catalytic Hydrogenation of Ketone (Câ•O) to Alcohol (OH) by Magnetite Nanoparticles Following Langmuir–Hinshelwood Kinetic Approach. ACS Applied Materials & Interfaces, 2015, 7, 6480-6489.	4.0	25
121	Effect of molar ratio of zinc nitrate: hexamethylenetetramine on the properties of ZnO thin film nanotubes and nanorods and the performance of dye-sensitized solar cell (DSSC). Journal of Materials Science: Materials in Electronics, 2015, 26, 7955-7966.	1.1	9
122	(001)-Faceted hexagonal ZnO nanoplate thin film synthesis and the heterogeneous catalytic reduction of 4-nitrophenol characterization. Journal of Alloys and Compounds, 2015, 650, 299-304.	2.8	33
123	Effect of ZnO growth time on the performance of dye-sensitized solar cell utilizing TiO2–ZnO core–shell nanograss hetero-structure. Materials Letters, 2015, 160, 388-391.	1.3	9
124	Effect of zinc acetate dihydrate precursor concentration on the properties of TiO 2 –ZnO core–shell nanograss hetero-structure. Journal of Alloys and Compounds, 2015, 623, 460-465.	2.8	10
125	Effect of bismuth telluride concentration on the thermoelectric properties of PEDOT:PSS–glycerol organic films. Physica E: Low-Dimensional Systems and Nanostructures, 2015, 66, 293-298.	1.3	15
126	Direct growth of oriented ZnO nanotubes by self-selective etching at lower temperature for photo-electrochemical (PEC) solar cell application. Journal of Alloys and Compounds, 2015, 618, 153-158.	2.8	74

#	Article	IF	CITATIONS
127	Effect of Growth Solution Concentration on the Performance of Boron Doped ZnO Dye-sensitized Solar Cell (DSSC). Journal of New Materials for Electrochemical Systems, 2015, 18, 213-218.	0.3	3
128	A high sensitive of an optical Raman sensor system to detect bisphenol A. , 2015, , 155-158.		1
129	Photo-polymerization of methacrylate based polymer electrolyte for dye-sensitized solar cell. Journal of Polymer Engineering, 2014, 34, 695-702.	0.6	5
130	Morphology, structure, optical property and photoelectrochemical property of TiO 2 nanoflower films synthesised via liquid phase deposition technique. Micro and Nano Letters, 2014, 9, 253-256.	0.6	3
131	Gold nanoplates as sensing material for plasmonic sensor of formic acid. , 2014, , .		1
132	Effect of organic dye on the performance of dye-sensitized solar cell utilizing TiO2 nanostructure films synthesized via CTAB-assisted liquid phase deposition technique. Russian Journal of Electrochemistry, 2014, 50, 1072-1076.	0.3	8
133	Synthesis of ZnO Nanorod Arrays by Chemical Solution and Microwave Method for Sensor Application. Key Engineering Materials, 2014, 605, 585-588.	0.4	3
134	Fabrication of ZnO Nanorod for Room Temperature NO Gas Sensor. Advanced Materials Research, 2014, 1043, 96-100.	0.3	1
135	Laser stimulated electrooptics in the Ag–ZnO nanorods. Physica E: Low-Dimensional Systems and Nanostructures, 2014, 61, 23-27.	1.3	12
136	Rapid synthesis of TiO2/MWCNTs nanocatalyst with enhanced photocatalytic activity using modified microwave technique. Materials Science in Semiconductor Processing, 2014, 25, 207-210.	1.9	19
137	ZnO nanocubes with (1 0 1) basal plane photocatalyst prepared via a low-frequency ultrasonic assisted hydrolysis process. Ultrasonics Sonochemistry, 2014, 21, 754-760.	3.8	46
138	Poriferous microtablet of anatase TiO2 growth on an ITO surface for high-efficiency dye-sensitized solar cells. Solar Energy Materials and Solar Cells, 2014, 122, 174-182.	3.0	40
139	Porous (001)-faceted Zn-doped anatase TiO ₂ nanowalls and their heterogeneous photocatalytic characterization. RSC Advances, 2014, 4, 57054-57063.	1.7	27
140	Highly-reactive AgPt nanofern composed of {001}-faceted nanopyramidal spikes for enhanced heterogeneous photocatalysis application. Journal of Materials Chemistry A, 2014, 2, 17655-17665.	5.2	42
141	Polymer electrolyte for photoelectrochemical cell and dye-sensitized solar cell: a brief review. Ionics, 2014, 20, 1201-1205.	1.2	16
142	Solvent controlled synthesis of CaO-MgO nanocomposites and their application in the photodegradation of organic pollutants of industrial waste. Russian Journal of Physical Chemistry A, 2014, 88, 836-844.	0.1	23
143	Effect of hexamethylenetetramines (HMT) surfactant concentration on the performance of TiO2 nanostructure photoelectrochemical cells. Russian Journal of Electrochemistry, 2014, 50, 974-980.	0.3	10
144	Enhancement of 1536nm emission of Er doped ZnO nanopowder by Ag doping. Optical Materials, 2014, 36, 1295-1298.	1.7	11

#	Article	IF	CITATIONS
145	Ag–ZnO Nanoreactor Grown on FTO Substrate Exhibiting High Heterogeneous Photocatalytic Efficiency. ACS Combinatorial Science, 2014, 16, 314-320.	3.8	34
146	Effect of Dye on the Performance of Nitrogen Doped TiO2 Solar Cell Prepared via Ammonia Treated Liquid Phase Deposition Technique. Journal of New Materials for Electrochemical Systems, 2014, 17, 033-037.	0.3	7
147	Formation of gold-coated multilayer graphene via thermal reduction. Materials Letters, 2013, 106, 200-203.	1.3	15
148	Modified microwave method for the synthesis of visible light-responsive TiO2/MWCNTs nanocatalysts. Nanoscale Research Letters, 2013, 8, 346.	3.1	27
149	Efficient Heterogeneous Catalytic Hydrogenation of Acetone to Isopropanol on Semihollow and Porous Palladium Nanocatalyst. ACS Applied Materials & Interfaces, 2013, 5, 9843-9849.	4.0	55
150	Preparation and Characterization of TiO ₂ Nanowire - Cu ₂ O Nanocube Composite Thin Film. Materials Science Forum, 2013, 756, 37-42.	0.3	1
151	Fibrous, ultra-small nanorod-constructed platinum nanocubes directly grown on the ITO substrate and their heterogeneous catalysis application. RSC Advances, 2013, 3, 19789.	1.7	26
152	Preparation of grass-like TiO2 nanostructure thin films: Effect of growth temperature. Applied Surface Science, 2013, 270, 109-114.	3.1	34
153	A molybdenum dithiolene complex as a potential photosensitiser for photoelectrochemical cells. International Journal of Hydrogen Energy, 2013, 38, 9578-9584.	3.8	9
154	H+, N+, and Ar+ ion irradiation induced structure changes of carbon nanostructures. New Carbon Materials, 2013, 28, 81-86.	2.9	13
155	Ultrafast Formation of ZnO Nanorods via Seed-Mediated Microwave Assisted Hydrolysis Process. Journal of Physics: Conference Series, 2013, 431, 012001.	0.3	6
156	Effect of organic dye, the concentration and dipping time of the organic dye N719 on the photovoltaic performance of dye-sensitized ZnO solar cell prepared by ammonia-assisted hydrolysis technique. Electrochimica Acta, 2013, 88, 639-643.	2.6	33
157	Deposition of Au/TiO2 Nanocomposite on ITO Surface by Seed-Mediated Liquid Phase Deposition Method. Journal of Physics: Conference Series, 2013, 431, 012011.	0.3	3
158	Ethanol sensor based on ZnO nanostructures prepared via microwave oven. , 2013, , .		7
159	Microwave Assisted Hydrothermal Method for Porous Zinc Oxide Nanostructured-Films. Journal of Nanoscience and Nanotechnology, 2013, 13, 2667-2674.	0.9	26
160	Preparation of patterned graphene-ZnO hybrid nanoflower and nanorods on ITO surface. , 2013, , .		0
161	Synthesis of silver nanosheets onto solid substrates by using seed-mediated growth method. , 2013, , .		0
162	Synthesis and Characterization of Gold Nanoplates onto Solid Substrates by Seed-Mediated Growth Method. Materials Science Forum, 2013, 756, 112-118.	0.3	0

#	Article	IF	CITATIONS
163	Effect of TiO <inf>2</inf> nanostructure's shape on the DSSCs performance. , 2013, , .		5
164	Visible light photocatalytic activity of TiO <inf>2</inf> /MWCNTs nanocomposite prepared using modified microwave technique. , 2013, , .		12
165	Formation of a Multi-Arm Branched Nanorod of ZnO on the Si Surface via a Nanoseed-Induced Polytypic Crystal Growth Using the Hydrothermal Method. Science of Advanced Materials, 2013, 5, 803-809.	0.1	13
166	Effect of Gold Nanoparticles Density Grown Directly on the Surface on the Performance of Organic Solar Cell. Current Nanoscience, 2013, 9, 187-191.	0.7	3
167	Effect of Ammonia and Zinc Acetate Precursor Concentration on the Morphology of ZnO Nanorods and the Performance of a ZnO Photoelectrochemical Cell. Current Nanoscience, 2013, 9, 730-736.	0.7	4
168	The 3rd ISESCO International Workshop and Conference On Nanotechnology 2012 (IWCN2012). Journal of Physics: Conference Series, 2013, 431, 011001.	0.3	1
169	Optimation growth of platinum and palladium nanoparticles on stainless steel 316L and activated carbon pellet substrates. AIP Conference Proceedings, 2012, , .	0.3	4
170	High sensitivity localized surface plasmon resonance sensor of gold nanoparticles: Surface density effect for detection of boric acid. , 2012, , .		5
171	The effects of mixed electroluminescent (EL) polymer layer thickness on the single layer organic light emitting diode (OLED) performance. , 2012, , .		1
172	Effect of TiO2 nanostructure morphology on the performance of a photoelectrochemical cell of ITO/TiO2/electrolyte/platinum. Journal of Solid State Electrochemistry, 2012, 16, 3947.	1.2	4
173	Silver nanocombs and branched nanowires formation in aqueous binary surfactants solution. Journal of Nanoparticle Research, 2012, 14, 1.	0.8	2
174	Localized Surface Plasmon Resonance sensor of Gold Nanoparticles for detection pesticides in water. , 2012, , .		2
175	Gold nanonetwork film on the ITO surface exhibiting one-dimensional optical properties. Nanoscale Research Letters, 2012, 7, 252.	3.1	8
176	Detection of Formaldehyde in Water: A Shape-Effect on the Plasmonic Sensing Properties of the Gold Nanoparticles. Sensors, 2012, 12, 10309-10325.	2.1	32
177	DEPTH-DEPENDENT TETRAGONAL DISTORTION STUDY OF AlGaN EPILAYER THIN FILM USING RBS AND CHANNELING TECHNIQUE. Modern Physics Letters B, 2012, 26, 1250086.	1.0	2
178	Effect of optical property of surfactant-treated TiO2 nanostructure on the performance of TiO2 photo-electrochemical cell. Journal of Solid State Electrochemistry, 2012, 16, 2005-2010.	1.2	14
179	Fluorescent and nonlinear optical features of CdTe quantum dots. Journal of Materials Science: Materials in Electronics, 2012, 23, 546-550.	1.1	22
180	Thermal Annealing Effect on the Morphology of Inkjet Printed Polymer:Fullerene Composites Solar Cells. Acta Physica Polonica A, 2012, 121, 155-157.	0.2	1

#	Article	IF	CITATIONS
181	Characterization of SnO ₂ Nanoparticles Prepared by Two Different Wet Chemistry Methods. Advanced Materials Research, 2011, 364, 322-326.	0.3	9
182	Photoinduced absorption of Ag nanoparticles deposited on ITO substrate. Journal of Alloys and Compounds, 2011, 509, S424-S426.	2.8	19
183	Growth of platinum nanoparticles on stainless steel 316L current collectors to improve carbon-based supercapacitor performance. Electrochimica Acta, 2011, 56, 10217-10222.	2.6	58
184	Optical features of the gold nanoparticles deposited on ITO substrates. Optics Communications, 2011, 284, 245-248.	1.0	9
185	A simple route to vertical array of quasi-1D ZnO nanofilms on FTO surfaces: 1D-crystal growth of nanoseeds under ammonia-assisted hydrolysis process. Nanoscale Research Letters, 2011, 6, 564.	3.1	18
186	The detection of pesticides in water using ZnCdSe quantum dot films. Advances in Natural Sciences: Nanoscience and Nanotechnology, 2011, 2, 025011.	0.7	15
187	Seed-Mediated Liquid Phase Deposition Method for TiO ₂ Nanostructure Growth on ITO Substrate: Effect of Surfactant. Advanced Materials Research, 2011, 364, 393-397.	0.3	8
188	Fabrication of Photoelectrochemical Cell Using Highly Compact Vertical Array ZnO Nanorod. Advanced Materials Research, 2011, 364, 293-297.	0.3	4
189	The effect of solvent on the morphology of an inkjet printed active layer of bulk heterojunction solar cells. Advances in Natural Sciences: Nanoscience and Nanotechnology, 2011, 2, 015014.	0.7	4
190	Dressing of Mwcnts with TiO ₂ Nanoparticles Using Modified Microwave Method. Advanced Materials Research, 2011, 364, 228-231.	0.3	7
191	The Optical Properties of Ammonia Treated TiO ₂ Nanostructure Prepared by Liquid Phase Deposition Method. Advanced Materials Research, 2011, 364, 470-474.	0.3	0
192	Effect of Organic Salt Doping Ratios on the Performance of Poly(9,9-di-n-hexylfluorenyl-2,7-diyl) Organic Light Emitting Diode, OLED. AIP Conference Proceedings, 2011, , .	0.3	3
193	Optical Electronic Nose Based on Fe (III) Complex of Porphyrins Films for Detection of Volatile Compounds. Key Engineering Materials, 2011, 495, 75-78.	0.4	1
194	Effect of ionic conductivity of a PAN–PC–LiClO4 solid polymeric electrolyte on the performance of a TiO2 photoelectrochemical cell. Journal of Solid State Electrochemistry, 2010, 14, 2089-2093.	1.2	6
195	Fabrication of a nanoparticle TiO2 photoelectrochemical cell utilizing a solid polymeric electrolyte of PAN–PC–LiClO4. Ionics, 2010, 16, 639-644.	1.2	10
196	Effect of the grain size of nanoparticle dye-coated titanium dioxide on the short-circuit current density and open-circuit voltage of an indium tin oxide/titanium dioxide/poly(acrylonitrile)-propylene carbonate-lithium perchlorate/graphite solar cell. Journal of Applied Polymer Science, 2010, 116, NA-NA.	1.3	1
197	Effective electrodeposition of Co–Ni–Cu alloys nanoparticles in the presence of alkyl polyglucoside surfactant. Applied Surface Science, 2010, 257, 1027-1033.	3.1	23
198	Physical, electrochemical and supercapacitive properties of activated carbon pellets from pre-carbonized rubber wood sawdust by CO2 activation. Current Applied Physics, 2010, 10, 1071-1075.	1.1	83

#	Article	IF	CITATIONS
199	The Effect of Donor:Acceptor Ratio on the Generated Photocurrent of Inkjet Printed Blended Poly (3-Octylthiophene-2.5-Diyl) and (6,6)-Phenyl C ₇₁ Butyric Acid Methyl Ester Bulk Heterojunction Organic Solar Cells. Materials Science Forum, 2010, 663-665, 823-827.	0.3	3
200	Detection of fungicide in water by ZnCdSe quantum dots thin film. , 2010, , .		0
201	Facile Approach for Preparing CdSeâ^•CdTe Heterostucture Quantum Dots. , 2010, , .		0
202	Effect of Organic Salt Doping on The Performance of Poly(9,9-di-n-hexylfluorenyl-2,7-diyl) Organic Light Emitting Diode, OLED. , 2010, , .		1
203	Fluorescence Properties of Hybrid CdTe Quantum Dots-Porphyrins Thin Films in Organic Vapors. , 2010, , .		0
204	The Dependence of Donor:Acceptor Ratio on the Photovoltaic Performances of Blended poly (3-octylthiophene-2,5-diyl) and (6,6)-phenyl C[sub 71] butyric acid methyl ester Bulk Heterojunction Organic Solar Cells. , 2010, , .		2
205	Facile Approach for Preparing CdSeâ^•CdTe Heterostucture Quantum Dots. , 2010, , .		0
206	Formation of Highly Thin, Electron-Transparent Gold Nanoplates from Nanoseeds in Ternary Mixtures of Cetyltrimethylammonium Bromide, Poly(vinyl pyrrolidone), and Poly(ethylene glycol). Crystal Growth and Design, 2010, 10, 3694-3698.	1.4	34
207	Optimizing of the inkjet printing technique parameters for fabrication of bulk heterojunction organic solar cells. , 2010, , .		2
208	Enhanced-photoluminescence properties of CdTe quantum dots prepared from the ternary surfactant mixture system. , 2010, , .		0
209	Localized surface plasmon resonance of gold nanoparticle-cytocrome C to detect the presence of nitric oxide gas. , 2010, , .		0
210	Highly red luminescence properties from ternary ZnCdTe quantum dots. , 2009, , .		2
211	Comparison of spherical nanogold particles and nanogold plates for the oxidation of dopamine and ascorbic acid. Journal of Electroanalytical Chemistry, 2009, 631, 58-61.	1.9	43
212	Synthesis and characterization of TiO2 nanoparticle films coated with organic dyes. Physica B: Condensed Matter, 2009, 404, 1420-1422.	1.3	5
213	Improvement of white organic light emitting diode performances by an annealing process. Thin Solid Films, 2009, 517, 4679-4683.	0.8	25
214	Formation of High-Yield Gold Nanoplates on the Surface: Effective Two-Dimensional Crystal Growth of Nanoseed in the Presence of Poly(vinylpyrrolidone) and Cetyltrimethylammonium Bromide. Crystal Growth and Design, 2009, 9, 2835-2840.	1.4	55
215	High-Yield Synthesis of Tetrahedral-Like Gold Nanotripods Using an Aqueous Binary Mixture of Cetyltrimethylammonium Bromide and Hexamethylenetetramine. Crystal Growth and Design, 2009, 9, 1146-1152.	1.4	45
216	Optical gas sensing selectivity property of ruthenium (II)-metalloporphyrins Langmuir–Blodgett films. Current Applied Physics, 2008, 8, 53-56.	1.1	10

#	Article	IF	CITATIONS
217	Electroluminescent from hybrid of Cdse quantum dot-organic light emitting diode. , 2008, , .		2
218	Synthesis of CdSe quantum dots: Effect of surfactant on the photoluminescence property. , 2008, , .		4
219	Fabrication of CdSe quantum dots-PHF organic hybrid light emitting diodes. , 2008, , .		Ο
220	Second order optical effects in Au nanoparticle-deposited ZnO nanocrystallite films. Nanotechnology, 2008, 19, 185709.	1.3	95
221	Synthesis of Palladium Nanobricks with Atomic-Step Defects. Crystal Growth and Design, 2008, 8, 1808-1811.	1.4	34
222	A Seed-Mediated Growth Method for Vertical Array of Single-Crystalline CuO Nanowires on Surfaces. Crystal Growth and Design, 2007, 7, 2404-2409.	1.4	57
223	Determination of methylprednisolone acetate in biological fluids at gold nanoparticles modified ITO electrode. Journal of Pharmaceutical and Biomedical Analysis, 2007, 44, 1147-1153.	1.4	12
224	Formation of Gold Nanoplates on Indium Tin Oxide Surface:  Two-Dimensional Crystal Growth from Gold Nanoseed Particles in the Presence of Poly(vinylpyrrolidone). Crystal Growth and Design, 2006, 6, 818-821.	1.4	93
225	Pump-dependent luminescence in the Ag nanoparticles doped by Erbium. Applied Surface Science, 2006, 253, 1626-1630.	3.1	9
226	A cast seed-mediated growth method for preparing gold nanoparticle-attached indium tin oxide surfaces. Applied Surface Science, 2006, 253, 2196-2202.	3.1	32
227	Attachment of gold nanoparticles onto indium tin oxide surfaces controlled by adding citrate ions in a seed-mediated growth method. Applied Surface Science, 2006, 253, 2933-2940.	3.1	32
228	An original planar multireflection system for sensing using the local surface plasmon resonance of gold nanospheres. Journal of Optics, 2006, 8, 268-271.	1.5	27
229	Influence of surface microstructure on optical response of ruthenium-porphyrins thin films gas sensor. EPJ Applied Physics, 2005, 29, 215-221.	0.3	8
230	Circularly polarized light-induced electrogyration in the Au nanoparticles on the ITO. Physica E: Low-Dimensional Systems and Nanostructures, 2005, 27, 420-426.	1.3	29
231	Acoustical circularly polarized gyration in the Au nanoparticles on the ITO. Physica E: Low-Dimensional Systems and Nanostructures, 2005, 28, 178-184.	1.3	10
232	Nonlinear optical properties of Au nanoparticles on indium–tin oxide substrate. Nanotechnology, 2005, 16, 1687-1692.	1.3	74
233	<title>Self-assembly layer of amino fluorenone derivative as optical receptor to detect cyclohexane
vapour</title> . , 2005, 5836, 461.		0
234	Control of the plasmon absorption of gold nanoparticles with a two-color excitation. Journal of Applied Physics, 2005, 98, 084304.	1.1	27

AKRAJAS ALI UMAR

#	Article	IF	CITATIONS
235	Growth of High-Density Gold Nanoparticles on an Indium Tin Oxide Surface Prepared Using a "Touch― Seed-Mediated Growth Technique. Crystal Growth and Design, 2005, 5, 599-607.	1.4	56
236	Circular acoustogyration effect on gold nanoparticles grown on indium tin oxide. Applied Optics, 2005, 44, 6905.	2.1	9
237	Self-assembled monolayer of copper(II) meso-tetra(4-sulfanatophenyl) porphyrin as an optical gas sensor. Sensors and Actuators B: Chemical, 2004, 101, 231-235.	4.0	23
238	Quartz crystal microbalance coated with poly-L-proline self-assembly layer to detect organic gases. , 2004, , .		3
239	Enriching the selectivity of metalloporphyrins chemical sensors by means of optical technique. Sensors and Actuators B: Chemical, 2002, 85, 191-196.	4.0	58
240	Optical sensing of capsicum aroma using four porphyrins derivatives thin films. Thin Solid Films, 2002, 417, 162-165.	0.8	33
241	Metalloporphyrins thin films as optical receptors for organic gases. , 0, , .		Ο
242	Non-Linear Optical Effects in Au Nanoparticle-Deposited ZnO Nanocrystalline Films. Journal of Nano Research, 0, 2, 31-38.	0.8	6
243	Recent Advances in Metal Nanoparticle-Attached Electrodes. , 0, , 297-318.		1
244	Plasmonic Responses of Gold Nanoparticles on Organic Vapor: Shape Effect. Materials Science Forum, 0, 663-665, 956-960.	0.3	0
245	Bright Photoluminescence of CdTe Quantum Dots Formed in Phosponic-Oleic Acids Binary Surfactants. Materials Science Forum, 0, 663-665, 25-28.	0.3	1
246	Fluorescence Gas Sensor Using CdTe Quantum Dots Film to Detect Volatile Organic Compounds. Materials Science Forum, 0, 663-665, 276-279.	0.3	9
247	The Effect of Nanoseed Concentration on the Aspect Ratio of Gold Nanorod. Advanced Materials Research, 0, 364, 254-259.	0.3	1
248	Detection of Formaldehyde Using Plasmonic Properties of Gold Nanoparticles . Key Engineering Materials, 0, 495, 79-82.	0.4	3
249	Synthesis of Monodisperse CdSe QDs Using Controlled Growth Temperatures. Advanced Materials Research, 0, 364, 485-488.	0.3	1
250	Study Phase Separation of Donor: Acceptor in Inkjet Printed Thin Films of Bulk Heterojunction Organic Solar Cells Using AFM Phase Imaging. Advanced Materials Research, 0, 364, 465-469.	0.3	3
251	Effect of ZnO Nanoseed Structure on the Growth Orientation of Vertical Array ZnO Nanorods via Hydrothermal Process. Applied Mechanics and Materials, 0, 229-231, 239-242.	0.2	3
252	Solvent Controlled Synthesis of Tin Oxide Nanocatalysts and their Applications in Photodegradation of Environmental Hazardous Materials. Materials Science Forum, 0, 756, 197-204.	0.3	9

#	Article	IF	CITATIONS
253	Localized Surface Plasmon Resonance Sensor Using Gold Nanoparticles for Detection of Bisphenol A. Key Engineering Materials, 0, 543, 342-345.	0.4	3
254	Localized Surface Plasmon Resonance Sensor of Gold Nanoplates for Detection of Boric Acid. Key Engineering Materials, 0, 605, 356-359.	0.4	4
255	Ag-Fe Alloy Nanoparticles Embedded in Polyaniline Nanocomposite Thin Films for <i>E. coli</i> Monitoring Sensor. Advanced Materials Research, 0, 1119, 101-105.	0.3	1
256	Synthesis and Characterization of PVA-Ag Doped Metals (Co, Al) Nanocomposite Thin Films Biosensors for Detection of <i>E. coli</i> in Water. Advanced Materials Research, 0, 1107, 706-711.	0.3	2
257	Fabrication and Characterization of PANI-Ag-Co Nanocomposite Thin Films as Microbial Sensor for <i>E. coli</i> Detection. Materials Science Forum, 0, 846, 641-649.	0.3	2
258	Synthesis of Blue-Luminescence Graphene Quantum Dots Using Hydrothermal Method. Solid State Phenomena, 0, 268, 259-263.	0.3	4
259	Performance of Dye-Sensitized Solar Cell Utilizing Ga-ZnO Nanorods: Effect of Ga Concentration. International Journal of Electrochemical Science, 0, , 7499-7506.	0.5	5
260	Two-Dimensional Transition Metal Dichalcogenide as Electron Transport Layer of Perovskite Solar Cells. , 0, , .		0